High Resolution Imaging of ISAR Based on Low Rank Matrix Denoising Technique

Yuanhang Tang, Yang Xu, Yongsheng Zhang

China Taiyuan Satellite Launch Center, Taiyuan, China

BOE Display Technology Co., Ltd, Hefei, China

yhtangt@mail.ustc.edu.cn, xuyanghf@boe.com.cn

Keywords: ISAR Imaging, Frequency Estimation, Matrix Enhancement and Matrix Pencil, Low Rank Matrix Denoising

Abstract: The problem of inverse synthetic aperture radar (ISAR) imaging can be expressed as a two-dimensional frequency estimation problem. Matrix enhancement and matrix pencil (MEMP) method is an effective frequency estimation method. This method belongs to the category of spectral estimation methods, and the performance of ISAR imaging using MEMP is sensitive to noise, which limits the application of this method in ISAR imaging. In the MEMP method, an enhanced matrix with a large dimension is first constructed according to the echo matrix. The enhanced matrix has low rank property when the scattering points in the imaging scene satisfy the sparse characteristic. Based on the low rank property of the enhanced matrix, we propose a denoising method for the MEMP. The simulation results prove that the proposed denoising method combining with the MEMP can achieve robust and effective high resolution imaging for ISAR.

1. Introduction

The inverse synthetic aperture radar (ISAR) imaging system has a uniform and dense filling in spatial spectral. In this case, the most common imaging method is the Fast Fourier Transform (FFT). According to the property of Fourier transform, the resolution ability of FFT method is limited by the range of spatial spectral filling. Therefore, the resolution of this method is limited, and high resolution imaging of radar system cannot be realized by FFT. In recent years, spectral estimation methods developed in array signal processing can achieve high resolution of direction of arrival estimation (DOA). Classical spectral estimation methods include MUSIC [2], ESPRIT [3], U-ESPRIT ([7], [9]) and Matrix Pencil ([4], [8]). In this paper, we use spectral estimation methods to achieve high resolution imaging of ISAR system. Spectral estimation methods can achieve high resolution imaging, but they are sensitive to noise. Therefore, an effective denoising technique is needed before using the spectral estimation method for imaging. In ISAR system, the target scattering coefficient is sparse in the imaging scene [5], resulting that the echo matrix is low rank. In this paper, denoising is performed according to the low rank property of the echo matrix, which reduces the sensitivity of the spectral estimation algorithm to noise.

2. ISAR signal model and MEMP method

ISAR is an important form of radar system. It can realize real-time high resolution imaging of moving targets, and has wide application value in the military field. The resolution of the ISAR system in the range dimension and cross range dimension are determined by bandwidth and accumulation angle respectively. The signal model in this paper is similar to the signal model in [9]. After compensation, the ISAR echo expression is:

$$y\left(f_m,\theta_n\right)=\iint_S \sigma\left(x,y\right)\exp\left\{-\mathrm{j}4\pi f_m\left(x\cos\theta_n+y\sin\theta_n\right)/c\right\}dxdy \tag{1}$$

Where S is the imaging area, $\sigma\left(x,y\right)$ is target scattering coefficient in position $\left(x,y\right)$. f_m is

  DOI: 10.25236/iwmecs.2019.003

sampled frequency points ($m=0,1,\cdots,M-1$) and θ_n is different look angles ($n=0,1,\cdots,N-1$). Therefore, $B=M\Delta f$ is the signal bandwidth, and $\Theta=N\Delta\theta$ is the cumulative observation angle. $\Delta f,\Delta\theta$ is the sampling interval for frequency and angle, respectively.

In the case of the far field, the angle θ_n is relatively small. Therefore, based on the approximation $\cos\theta_n\approx 1$, $\sin\theta_n=\theta_n$. The echo can be approximated as:

$$y(f_m,\theta_n)\approx\iint_S\sigma(x,y)\exp\{-\mathrm{j}4\pi xf_m/c-\mathrm{j}4\pi\theta_n f_m y/c\}\,dxdy \tag{2}$$

When the system bandwidth is limited, there is $f_m/c\approx f_0/c=1/\lambda_0$. Therefore, the above echo can be further expressed as:

$$y(f_m,\theta_n)=\iint_S e^{-\mathrm{j}4\pi\frac{f_m}{c}x}\sigma(x,y)e^{-\mathrm{j}4\pi\frac{\theta_n}{\lambda_0}y}\,dxdy \tag{3}$$

By meshing the imaging area discretely, the echo data can be written as a matrix form:

$$\mathbf{Y}=\mathbf{A}_x\boldsymbol{\sigma}\mathbf{A}_y^H \tag{4}$$

The echo matrix $\mathbf{Y}$ has a dimension of $M\times N$. $\boldsymbol{\sigma}$ is scattering coefficient matrix, and the dimension is $P\times Q$. The scattering coefficient at its position (x_p,y_q) is $\sigma_{pq}=\sigma(x_p,y_q)$.

Define the spatial spectrum filling form of ISAR system as:

$$\begin{cases}k_x^m=2f_m/c\\ k_y^n=2\theta_n/\lambda_0\end{cases} \tag{5}$$

The echo can be further rewritten as:

$$y(f_m,\theta_n)=\iint_S\sigma(x,y)\exp\left\{-\mathrm{j}2\pi\left(k_x^m x+k_y^n y\right)\right\}dxdy \tag{6}$$

According to the spatial spectral filling form, the spatial spectral filling range in x and y direction is $\Delta K_x=2B/c$ and $\Delta K_y=2\Theta/\lambda_0$, respectively. Then the resolution in range and cross range dimension is:

$$\begin{cases}\rho_x=1/\Delta K_x=c/2B\\ \rho_y=1/\Delta K_y=\lambda_0/2\Theta\end{cases} \tag{7}$$

It can be concluded that in the ISAR imaging system, the spatial spectral filling is dense and uniform. The imaging resolution reconstructed by the FFT method is limited by the spatial spectral filling range of the system.

As previously mentioned, the spatial spectral filling is dense and uniform in ISAR system. So spectral estimation method can be using to overcome the resolution limitation by FFT. MEMP (Matrix Enhancement and Matrix Pencil) is a two-dimensional frequency estimation method. Firstly, the Enhanced matrix is constructed according to the echo matrix, and then the two-dimensional frequency is estimated by using the matrix pencil method, thereby estimating the position of scattering points. You can get more details about this method in [8].

3. Denoising Technique Based on Low Rank Property

As we all know, the matched filtering (MF) algorithm is the most common denoising method, and this method has a universal performance for the denoising problem. In ISAR imaging, the target will exhibit sparse characteristics in space, that is, the number of strong scattering points is limited. This means that in the scattering coefficient matrix $\boldsymbol{\sigma}$, the scattering coefficient is non-zero only at a few positions, which results in the echo matrix $\mathbf{Y}$ having low rank property. If the low rank echo

matrix is denoised by the matched filtering method, a certain denoising performance will be obtained, but is not obvious. Matched filtering is a universal denoising method, it does not considered the low rank property of the echo matrix. In recent years, low rank matrix recovery technique has been widely used in image denoising. Many low rank matrix restoration algorithms have been proposed by domestic and foreign researchers ([10], [12]). The core idea of the denoising method based on the low rank property of the matrix is that when the matrix satisfies the low rank property, there is a strong correlation between the matrix elements. When the low rank matrix is contaminated by noise, there is little correlation between the noise matrix elements. The low rank denoising method uses the difference between the low rank matrix elements and the noise matrix elements to achieve an improvement in SNR.

3.1 Matched Filtering Deniosing

Assuming that the echo data is contaminated by noise, the noisy echo is expressed as:

$$\mathbf{Y}_n = \mathbf{A}_x \boldsymbol{\sigma} \mathbf{A}_y^H + \mathbf{N} \tag{8}$$

For the noisy echo matrix $\mathbf{Y}_n$, we can obtain the matrix with the enhanced SNR after matched filtering:

$$\tilde{\mathbf{Y}}_n = \mathbf{A}_x^H \mathbf{Y}_n \mathbf{A}_y = \tilde{\mathbf{Y}} + \mathbf{A}_x^H \mathbf{N} \mathbf{A}_y = \mathbf{A}_x^H \mathbf{A}_x \boldsymbol{\sigma} \mathbf{A}_y^H \mathbf{A}_y + \mathbf{A}_x^H \mathbf{N} \mathbf{A}_y \tag{9}$$

The enhanced SNR after matched filtering is:

$$\mathrm{SNR} = 10 \lg \left(\left\| \mathbf{A}_x^H \mathbf{A}_x \boldsymbol{\sigma} \mathbf{A}_y^H \mathbf{A}_y \right\|_F^2 \Big/ \left\| \mathbf{A}_x^H \mathbf{N} \mathbf{A}_y \right\|_F^2 \right) \tag{10}$$

After matched filtering, the low rank echo matrix changes into $\mathbf{A}_x^H \mathbf{A}_x \boldsymbol{\sigma} \mathbf{A}_y^H \mathbf{A}_y$, which still has low rank property. Therefore, a deeper denoising can be performed using the low rank property of the matrix.

3.2 Denoising methods based on matrix low rank property

When the matrix satisfies the low rank property, the denoising problem can be expressed as [5]:

$$\min_{\tilde{\mathbf{Y}}} \operatorname{rank}\left(\tilde{\mathbf{Y}} \right) \quad s.t. \ \left\| \tilde{\mathbf{Y}}_n - \tilde{\mathbf{Y}} \right\|_F^2 \le \delta \tag{11}$$

Since the rank of the matrix is the same as the number of non-zero singular value of the matrix, the rank constraint of the matrix can be equivalent to the l_0 norm constraint of the matrix singular value. That is, the constraint problem of the above formula becomes:

$$\min_{\tilde{\mathbf{Y}}} \left\| \sigma\left(\tilde{\mathbf{Y}} \right) \right\|_0 \quad s.t. \ \left\| \tilde{\mathbf{Y}}_n - \tilde{\mathbf{Y}} \right\|_F^2 \le \delta \tag{12}$$

Where, $\sigma\left(\tilde{\mathbf{Y}} \right)$ represents one-dimensional singular value vector of the matrix $\tilde{\mathbf{Y}}$. $\|*\|_F$ represents Frobenious norm.

Regardless of the rank constraint or l_0 norm constraint of the matrix singular value, the optimization problem is NP-hard, and it is impossible to solve specificly. The most general solution is convex relaxation.Then the l_0 norm constraint of the matrix singular value becomes kernel norm constraint (KNC). The optimization problem can be expressed as:

$$\min_{\tilde{\mathbf{Y}}} \left\| \sigma\left(\tilde{\mathbf{Y}} \right) \right\|_* \quad s.t. \ \left\| \tilde{\mathbf{Y}}_n - \tilde{\mathbf{Y}} \right\|_F^2 \le \delta \tag{13}$$

Where, $\left\| \sigma\left(\tilde{\mathbf{Y}} \right) \right\|_*$ the kernel norm of the matrix which is defined as the sum of all singular values of the matrix $\tilde{\mathbf{Y}}$.

After convex relaxation,the optimization problem can be solved by the convex optimization

method and a global optimal solution can be obtained easily. However, the method of convex relaxation will lead to a large deviation between the obtained solution and the real solution. The fundamental reason is that the kernel norm can not describe the low rank property of the matrix precisely. In order to get more accurate solution, various non-convex constraints are used to approximate the rank constraint of the matrix. In [5], a low rank matrix denoising method based on hyperbolic tangent constraint (HTC) is studied.

After the non-convex hyperbolic tangent constraint, the denoising problem becomes the following constraint optimization problem:

$$\min_{\tilde{\mathbf{Y}}} \sum_i g_\gamma\left(\sigma_i\left(\tilde{\mathbf{Y}}\right)\right) \quad s.t. \ \left\|\tilde{\mathbf{Y}}_n - \tilde{\mathbf{Y}}\right\|_F^2 \le \delta \tag{14}$$

Where, $g_\gamma(\cdot)$ represents hyperbolic tangent function. The author in [5] uses a two-layer loop to solve such optimization problem.

In this paper, we use iterative method to solve this problem. The denoising problem can be expressed as:

$$\min_{\mathbf{W},\mathbf{V}} \frac{1}{2}\left\|\mathbf{WV} - \mathbf{Z}\right\|_F^2 \ s.t. \left\|\mathbf{Z} - \tilde{\mathbf{Y}}_n\right\|_F^2 \le \delta \tag{15}$$

Where $\mathbf{Z}$ is the auxiliary matrix. It has the same dimension as $\tilde{\mathbf{Y}}_n$. In practice, we can estimate the number of scattering points in the scene according to the Gerschgorin disk criterion [11], and then we can obtain the rank of the pure echo matrix $\mathbf{Y}$. So the rank of the matrix $\tilde{\mathbf{Y}}_n$ is as same as the number of scattering points, i.e. $rank\left(\tilde{\mathbf{Y}}\right) = K$. Then the dimension of matrix $\mathbf{W}$ is $P \times K$, and the dimension of matrix $\mathbf{V}$ is $K \times Q$. δ is a parameter related to the noise level. Due to the sparsity of scattering points in the scene, K is much smaller than P and Q.

To solve this optimization problem, iterative Gauss-Seidel method will be commonly used [10]. In each iteration of the GS method, other variables are fixed and known, and one variable is minimized. For example, if $\mathbf{Z}$ and $\mathbf{V}$ is known, then the solution of $\mathbf{W}$ becomes:

$$\mathbf{W}_+ \leftarrow \mathbf{ZV}^\dagger = \arg\min_{\mathbf{W}\in\mathbb{C}^{P\times K}} \frac{1}{2}\left\|\mathbf{WV} - \mathbf{Z}\right\|_F^2 \tag{16}$$

Where † represents the Moore-Penrose inverse matrix.

Therefore, the iterative process of the GS method can be expressed as following:

$$\begin{aligned} \mathbf{W}_+ &\leftarrow \mathbf{ZV}^\dagger = \mathbf{ZV}^T\left(\mathbf{VV}^T\right)^{-1} \\ \mathbf{V}_+ &\leftarrow \left(\mathbf{W}_+\right)^\dagger \mathbf{Z} = \left(\mathbf{W}_+^T\mathbf{W}_+\right)^{-1}\left(\mathbf{W}_+^T\mathbf{Z}\right) \\ \mathbf{Z}_+ &\leftarrow \mathbf{W}_+\mathbf{V}_+ \end{aligned} \tag{17}$$

When the GS method is used to solve the low rank matrix with larger dimension iteratively, the convergence speed of the algorithm is much slower. We have improved the GS method by weighting the current value with the value of the GS method in each iteration of the step to ensure fast convergence of the algorithm. The iterative process of the algorithm is:

$$
\begin{aligned}
&\mathbf{W}_{+} \leftarrow \mathbf{Z}\mathbf{V}^{T}\left(\mathbf{V}\mathbf{V}^{T}\right)^{-1} \\
&\mathbf{W}_{+}(\omega) \leftarrow \omega\mathbf{W}_{+}+(1-\omega)\mathbf{W} \\
&\mathbf{V}_{+} \leftarrow \left(\mathbf{W}_{+}^{T}(\omega)\mathbf{W}_{+}(\omega)\right)^{-1}\left(\mathbf{W}_{+}^{T}(\omega)\mathbf{Z}\right) \\
&\mathbf{V}_{+}(\omega) \leftarrow \omega\mathbf{V}_{+}+(1-\omega)\mathbf{V} \\
&\mathbf{Z}_{+}(\omega) \leftarrow \mathbf{W}_{+}(\omega)\mathbf{Z}_{+}(\omega)
\end{aligned}
\tag{18}
$$

Where $\omega \geq 1$, when ω=1 the iterative method is the GS method. Due to $\omega > 1$, the influence of the current value on the iterative result is a negative contribution during the iterative process, so the forgetting speed of the current value will be faster, thus speeding up the convergence speed of the algorithm.

4. Simulation Quasi Real Data Result

The rank of the matrix is closely related to the singular value of the matrix. We first compare the three kinds of denoising algorithms, i.e. kernel norm constraint (KNC) denoising, hyperbolic tangent constraint (HTC) denoising and iterative denoising, using the singular value distribution of signal matrix and noise matrix. The ISAR echo data is generated firstly, and the simulation parameters are shown in table 1. In simulation, we assume that the scene satisfies the sparsity, that is, the number of non-zero scattering coefficients in the scene is relatively small compared to the number of discrete grids. Therefore, the echo matrix has a low rank property.

Table 1.Simulation parameters of ISAR system

center frequency	10GHz	size of scence	6m×6.8m
points of frequency	100	points of angle	100
bandwidth	1GHz	cumulative angle	5°
number of grids in x	201	number of grids in y	201

After generating the echo data, Gaussian noise with SNR of 0dB is added to the echo matrix, and the singular value distribution of the pure echo matrix and the noise matrix is obtained by the singular value decomposition (SVD), as shown by the black and yellow lines in figure 1. It can be seen that there is a significant difference of SV between the signal matrix and the noise matrix. This difference reflects the correlation of the matrix elements. If the SV distribution curve of the noise matrix is closer to the SV distribution curve of the signal matrix after denoising, the denoising performance of this algorithm is better.

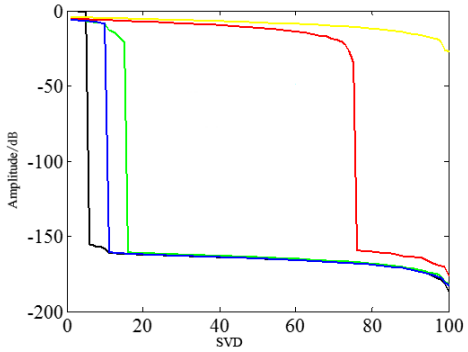

Figure 1. SV distribution curve of different denoising methods

After denoising by the kernel norm constraint denoising method, the SV distribution of the noise is shown by the red line in Figure 1. It can be seen that after this denoising method, there is still a big gap between the SV distribution of the noise and signal. After denoising by the hyperbolic tangent constraint denoising method, the SV distribution of the noise is shown by the green line. In

this case, the SV distribution of the noise is closer to the signal, so the denoising performance has been greatly improved comparing with the red line. The blue line shows the SV distribution curve of noise after denoising using proposed iterative denoising method. The curve is closest to the SV distribution of the signal than the other two methods, so it has the best denoising performance.

We compare the performance of the three denoising methods using Monte Carlo simulation to eliminate random error. The results are shown in the figure 2. Figure 2(a) is the curve of the echo SNR after denoising changing with the original echo SNR. In this simulation, the rank of the echo matrix is set to 5. We use 1000 Monte Carlo simulations to average the denoising performance. Figure 2(b) is a plot of the echo SNR as a function of matrix rank after denoising. In this simulation, the original echo SNR is set to 5dB, and the Monte Carlo simulation method is also used.

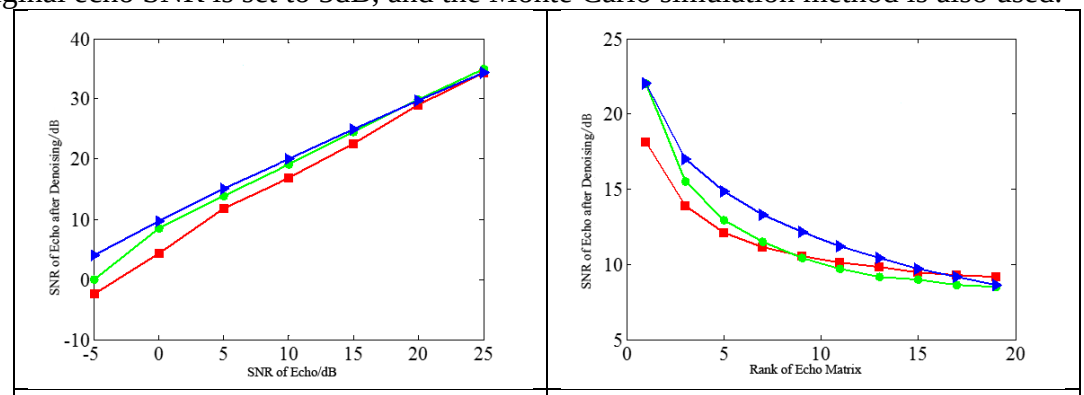

(a) (b)

Figure 2. Denoising performance of different methods

The simulation of B-727 quasi real data is also performed. The Gaussian white noise with SNR of 5 dB is added to the original data, and the imaging results after denoising by matched filtering and the other three low rank denoising algorithms are shown in figure 3.

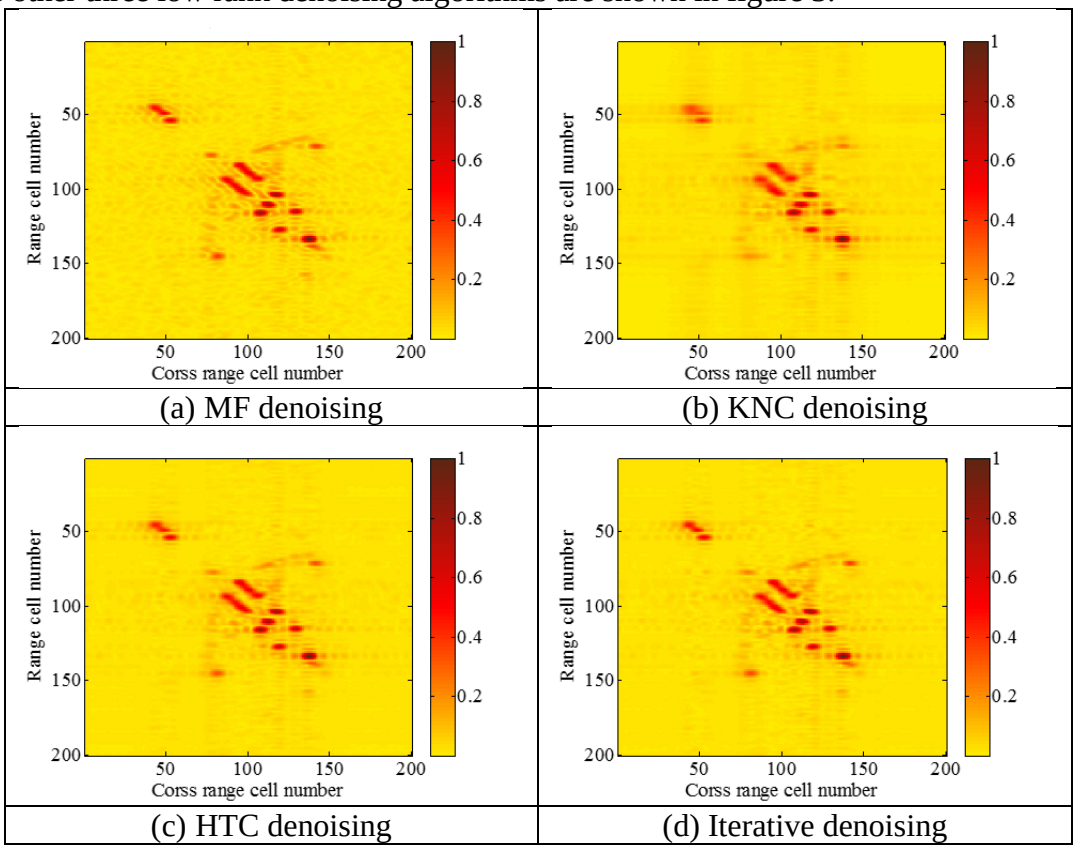

(a) MF denoising (b) KNC denoising

(c) HTC denoising (d) Iterative denoising

Figure 3. Imaging results of B-722 using different denoising methods

It can be seen from the results that the kernel norm constraint can not approximate the rank constraint well, so the solution is not the optimal solution and the error is very large. Hyperbolic tangent constraint denoising and the the iterative denoising algorithm proposed in this paper have similar performance visually. The denoising performance of the three algorithms is given from the perspective of image entropy (IE) and image contrast (IC) quantitatively in table 2. It can be seen that the performance of iterative denoising is the best.

Table 2. Performance comparison of different denoising methods

		MF	KNC denoising	HTC denoising	iterative denoising
B-727	IE	7.8309	7.9548	7.5452	**7.5394**
	IC	6.9641	6.8534	7.2755	**7.2781**

Finally, we combine the proposed denoising technique with spectral estimation method MEMP. The estimation results of the scattering points before and after denoising are shown in figure 4.

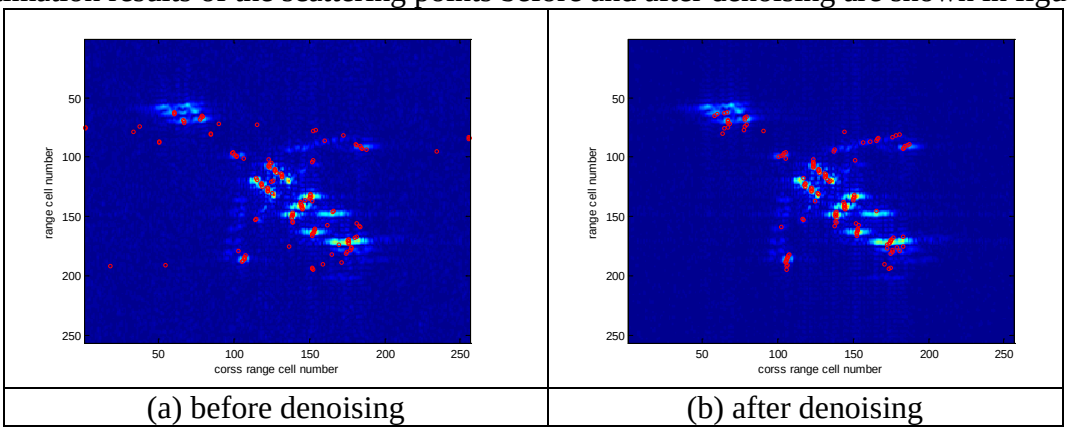

(a) before denoising (b) after denoising

Figure 4. Imaging results of B-722 using MEMP and iterative denoising technique

The red circle is the position estimation results of scattering points. The background is the result obtained by the FFT method. It can be seen that the MEMP method is more accurate in estimating the position of the scattering points after the denoising, and its resolution performance is better than FFT method. So MEMP combining with our proposed iterative denoising technique can realize robust and effective high resolution imaging for ISAR.

5. Conclusion

The sensitivity of matrix enhancement and matrix pencil method to noise is illustrated in this paper. The denoising method based on the low rank property of the matrix is introduced, and the performance of various denoising methods is compared. Finally, the proposed denoising method is combined with the MEMP method to realize a robust high-resolution imaging technique.

References

[1] Z. Bao, M. D. Xing, “Radar Imaging Technique,” Electronic Industry Press, 2005.
[2] J. W. Odendaal, E. Barnard, W. I. Pistorius, “Two dimensional high resolution radar imaging using the MUSIC algorithm,” IEEE Transactions on Antennas and Propagation, vol. 42, no. 10, pp. 1386-1391, 1994.
[3] R. Roy, T. Kailath, “ESPRIT-estimation of signal parameters via rotational invariance techniques,” IEEE Transactions on Acoustics, Speech, and Signal Processing, vol. 37, no. 7, pp. 984-995, 1989.
[4] Y. Hua, T. K. Sarkar, “Matrix pencil method for estimating parameters for exponentially dampediundamped rinuso ds in noise,” IEEE Transactions on Acoustics, Speech, and Signal Processing, vol. 36, no. 5, pp. 814-824, 1990.
[5] X. F. Lu, “Research on MIMO radar imaging for sparse distribution target,” Doctoral

dissertation, University of Science and Technology of China, 2017.
[6] G. H. Golub, C. F. Van Loan: Matrix computations. In: Johns Hopkins Studies in the Mathematical Sciences, 3rd edn. Johns Hopkins University Press, Baltimore (1996).
[7] X. Wang, M. Zhang, J. Zhao, “Super-resolution ISAR imaging via 2D unitary ESPRIT,” Electronics Letters, vol. 51, no. 6, pp. 519-521, 2015.
[8] Y. Hua, “Estimating two-dimensional frequencies by matrix enhancement and matrix pencil,” IEEE Transactions on Signal Processing, vol. 40, no. 9, pp. 2267-2280, 1992.
[9] J. Zhao, M. Zhang, X. Wang, Z. Cai, D. Nie, “Three-dimensional super resolution ISAR imaging based on 2D unitary ESPRIT scattering centre extraction technique,” IET Radar, Sonar & Navigation, vol. 11, no. 1, pp. 98-106, 2017.
[10] Z. Wen, W. Yin, Y. Zhang, “Solving a low-rank factorization model for matrix completion by a nonlinear successive over-relaxation algorithm,” Mathematical Programming Computation, vol. 4, no. 4, pp. 333-361, 2012.
[11] H. T. Wu, J. F. Yang, F. K. Chen, “Source number estimators using transformed gerschgorin radii,” IEEE Transactions on Signal Processing, vol. 43, no. 6, pp. 1325-1333, 1995.
[12] J. R. Shi, X. Y. Zheng, “Advances in Matrix Completion Algorithms,” vol. 41, no. 4, pp. 13-20, 2014.